CENTRE FOR **STOCHASTIC GEOMETRY**
AND ADVANCED **BIOIMAGING**

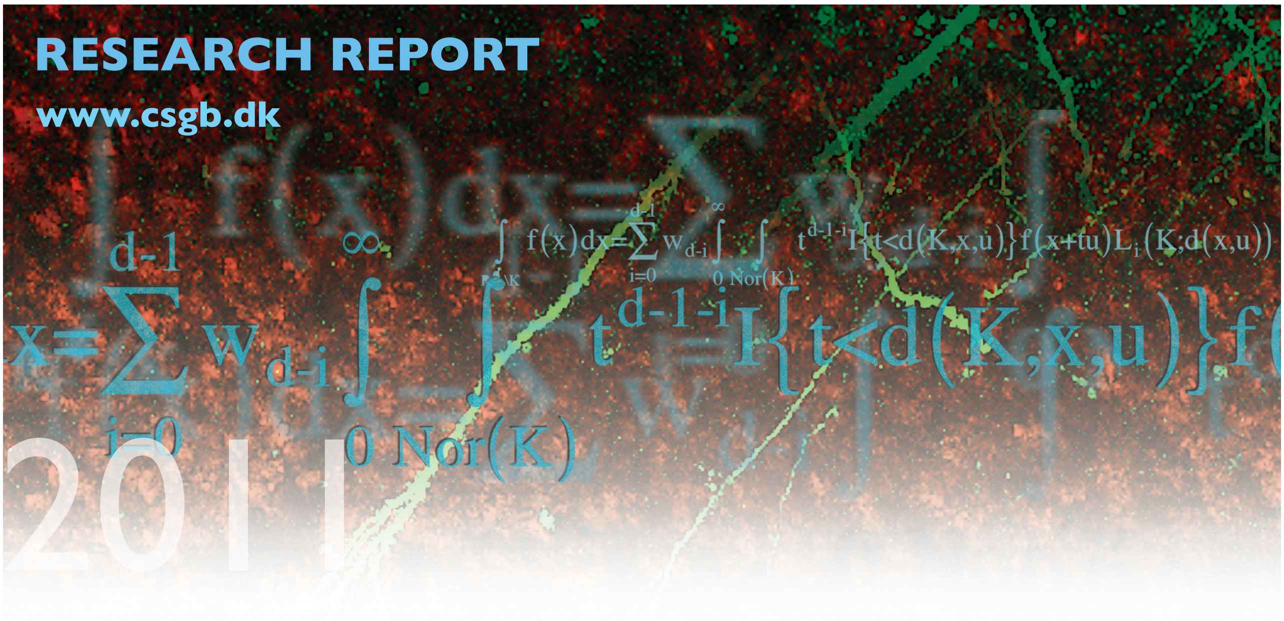

Linda V. Hansen, Thordis L. Thorarinsdottir and Tilmann Gneiting

Lévy particles:
Modelling and simulating star-shaped random sets

No. 04, September 2011

Lévy particles: Modelling and simulating star-shaped random sets

Linda V. Hansen[1], Thordis L. Thorarinsdottir[2] and Tilmann Gneiting[2]

[1]Department of Mathematical Sciences, Aarhus University, Denmark
[2]Institute of Applied Mathematics, University of Heidelberg, Germany

Abstract

Lévy particles provide a flexible framework for modelling and simulating three-dimensional star-shaped random sets. The radial function of a Lévy particle arises from a kernel smoothing of a Lévy basis, and is associated with an isotropic random field on the sphere. If the kernel is proportional to a von Mises–Fisher density, or uniform on a spherical cap, the correlation function of the associated random field admits a closed form expression. Using a Gaussian basis, the fractal or Hausdorff dimension of the surface of the Lévy particle reflects the decay of the correlation function at the origin, as quantified by the fractal index. Under power kernels we obtain particles with boundaries of any Hausdorff dimension between 2 and 3.

Keywords: celestial body; correlation function; Hausdorff dimension; Lévy basis; random field on a sphere; simulation of star-shaped random sets

1 Introduction

Mathematical models for three-dimensional particles have received great interest in astronomy, botany, geology, material science and zoology, among many other disciplines. Early approaches include that of Wicksell (1925, 1926), who addressed the estimation of the number and the size distribution of three-dimensional corpuscles in biological tissue from planar sections. He proposed both a spherical model and a more flexible ellipsoidal model. Wicksells's ideas were elaborated half a century later by Cruz-Orive (1976, 1978), who studied more general particle size-shape distributions in both continuous and discrete settings.

While some particles such as crystals have a rigid shape, many real-world objects are star-shaped, highly structured and stochastically varying. As a result, flexible yet parsimonious models for star-shaped random sets have been in high demand. Grenander and Miller (1994) proposed a model for two-dimensional featureless objects with no obvious landmarks, which are represented by a deformed polygon along with a Gaussian shape model. This was investigated further in Kent et al. (2000)

Corresponding author: Linda V. Hansen, lvh@imf.au.dk

and Hobolth et al. (2002), and a non-Gaussian extension was suggested by Hobolth et al. (2003). Miller et al. (1994) proposed an isotropic deformation model that relies on spherical harmonics and was studied by Hobolth (2003), where it was applied to monitor tumour growth. A related Gaussian random shape model was studied by Muinonen et al. (1996) and used by Muñoz et al. (2007) to represent Saharan desert dust particles.

In this paper we propose a flexible framework for modelling three-dimensional star-shaped particles, where the radial function is a random field on the sphere that arises through a kernel smoothing of a Lévy basis. Specifically, let $Y \subset \mathbb{R}^3$ be a three-dimensional compact set, which is star-shaped with respect to an interior point o. Then there is a one-to-one correspondence between the set Y and its radial function $X = \{X(u) : u \in \mathbb{S}^2\}$, where

$$X(u) = \max\{r \geq 0 : o + ru \in Y\}, \qquad u \in \mathbb{S}^2,$$

with $\mathbb{S}^2 = \{x \in \mathbb{R}^3 : \|x\| = 1\}$ denoting the unit sphere in $\mathbb{R}^3$. We model X as a real-valued random field on $\mathbb{S}^2$ via a kernel smoothing of a Lévy basis, in that

$$X(u) = \int_{\mathbb{S}^2} K(v, u)\, \Gamma(\,\mathrm{d}v), \qquad u \in \mathbb{S}^2, \tag{1.1}$$

where $K : \mathbb{S}^2 \times \mathbb{S}^2 \to \bar{\mathbb{R}}$ is a suitable kernel function, and Γ is a Lévy basis on the Borel subsets of $\mathbb{S}^2$, that is, an infinitely divisible and independently scattered random measure. If X is a nonnegative process, the random particle can be described as the set

$$Y = \bigcup_{u \in \mathbb{S}^2} \{o + ru : 0 \leq r \leq X(u)\} \subset \mathbb{R}^3, \tag{1.2}$$

so that the particle contains the centre o, which without loss of generality can be assumed to be the origin, and the distance in direction u from o to the particle boundary is given by $X(u)$. A potentially modified particle Y_c arises in the case of a general, not necessarily nonnegative process, where we replace $X(u)$ by $X_c(u) = \max(c, X(u))$ for some $c > 0$. We call Y or Y_c a Lévy particle, with realisations being illustrated in Figure 1. The Lévy particle framework is a special case of the linear spatio-temporal Lévy model proposed by Jónsdóttir et al. (2008) in the context of tumour growth. Alternatively, it can be seen as a generalisation and a three-dimensional extension of the model proposed in Hobolth et al. (2003), while also being a generalisation of the Gaussian random shape models of Miller et al. (1994) and Muinonen et al. (1996).

The realisations in Figure 1 demonstrate that the boundary or surface of a Lévy particle allows for regular as well as irregular behaviour. The roughness or smoothness of the surface in the limit as the observational scale becomes infinitesimally fine can be quantified by the fractal or Hausdorff dimension, which for a surface in $\mathbb{R}^3$ varies between 2 and 3, with the lower limit corresponding to a smooth, differentiable surface, and the upper limit corresponding to an excessively rough, space-filling surface (Falconer, 1990). The concept dates back to Hausdorff (1919) and has attracted much attention due to the work of Mandelbrot, who argued that fractal objects and surfaces are ubiquitous in nature (Mandelbrot, 1982). Under a Gaussian Lévy basis,

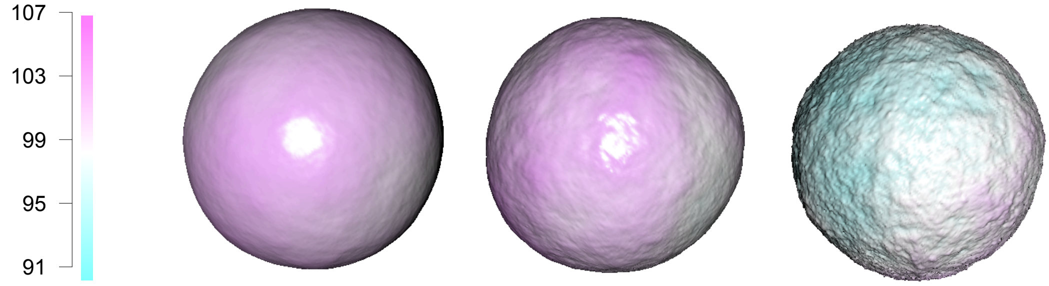

Figure 1: Lévy particles with mean $\mu_X = 100$ and variance $\sigma_X^2 = 10$, using a Gaussian Lévy basis and the power kernel (4.5) with $q = 0.05$ (left), $q = 0.25$ (middle) and $q = 0.5$ (right). The fractal or Hausdorff dimension of the particle surface equals $2 + q$.

the Hausdorff dimension of the surface of an isotropic Lévy particle is determined solely by the behaviour of the correlation function of the associated random field on the sphere. We investigate the properties of Lévy particles under parametric families of isotropic kernel functions, including power kernels, and kernels that are proportional to von Mises–Fisher densities, or uniform on spherical caps. Power kernels generate Gaussian Lévy particles which surface can attain any Hausdorff dimension between 2 and 3. Von Mises–Fisher and uniform kernels generate Gaussian particles with boundaries of Hausdorff dimension 2 and 2.5, respectively.

The remainder of the paper is organised as follows. Section 2 recalls basic properties of Lévy bases and of the radial function in the Lévy particle model (1.1). In Section 3 we show how to derive the Hausdorff dimension of an isotropic Gaussian Lévy particle from the infinitesimal behaviour of the correlation function of the underlying random field at the origin. Section 4 introduces the aforementioned families of isotropic kernels and discusses the properties of the associated correlation functions and Lévy particles. Section 5 presents a simulation algorithm and simulation examples, including a case study on celestial bodies and a discussion of planar Lévy particles. The paper ends with a discussion in Section 6.

2 Preliminaries

The properties of the random function (1.1) that characterises a Lévy particle process depend both on the kernel function K and the Lévy basis Γ. For the Lévy basis, we use two of the types considered by Jónsdóttir et al. (2008). Specifically, we assume Γ to be either a Gaussian Lévy basis with parameters $\mu \in \mathbb{R}$ and $\sigma^2 > 0$, so that

$$\Gamma(A) \sim \mathcal{N}\big(\mu\,\lambda(A), \sigma^2\lambda(A)\big), \tag{2.1}$$

or a gamma Lévy basis with shape $\kappa > 0$ and rate $\tau > 0$, so that

$$\Gamma(A) \sim \mathrm{Gamma}(\kappa\,\lambda(A), \tau), \tag{2.2}$$

where $\lambda(A)$ denotes the surface measure of a Borel set $A \subseteq \mathbb{S}^2$, with $\lambda(\mathbb{S}^2) = 4\pi$. We assume that the kernel function K is isotropic, in that $K(v, u) = k(d(v, u))$ depends on the points $v, u \in \mathbb{S}^2$ through their great circle distance $d(v, u) \in [0, \pi]$

Table 1: Mean and variance parameters for Gaussian and gamma bases for the Lévy particle process.

Lévy basis Γ	μ_Γ	σ^2_Γ
Normal	μ	σ^2
Gamma	κ/τ	κ/τ^2

only. As $\cos d(v,u) = u \cdot v$, this is equivalent to assuming that the kernel depends on the inner product $u \cdot v$ only. Results of Jónsdóttir et al. (2008) in concert with the rotation invariance in the isotropic case imply that the mean function $\mathbb{E}(X(u))$ and the variance function $\mathrm{Var}(X(u))$ are constant, that is,

$$\mu_X = \mathbb{E}(X(u)) = \mu_\Gamma \, c_1 \qquad \text{and} \qquad \sigma^2_X = \mathrm{Var}(X(u)) = \sigma^2_\Gamma \, c_2$$

for $u \in \mathbb{S}^2$, where we assume that

$$c_n = \int_{\mathbb{S}^2} k(d(v,u))^n \; \mathrm{d}v$$

is finite for $n = 1, 2$. The values of the mean and variance parameters μ_Γ and σ^2_Γ depend on the Lévy basis, as summarised in Table 1. Depending on the choice of the Lévy basis, $X(u)$ might not be positive and thus may not be usable for determining distances. We then use the cut-off version $X_c(u) = \max(c, X(u))$ for $c > 0$, which generates the random particle Y_c. For further discussion of the relevant properties of Lévy bases see Hellmund et al. (2008).

Note that X can be interpreted as a stochastic process on the sphere (Jones, 1963), whose covariance function is given by

$$\mathrm{Cov}(X(u_1), X(u_2)) = \sigma^2_\Gamma \int_{\mathbb{S}^2} k(d(v,u_1)) \, k(d(v,u_2)) \; \mathrm{d}v, \qquad u_1, u_2 \in \mathbb{S}^2,$$

Under an isotropic kernel, the random field X is stationary and isotropic, and it is readily seen that $\mathrm{Corr}(X(u_1), X(u_2)) = C(d(u_1,u_2))$, where

$$C(\theta) = \frac{2}{c_2} \int_0^\pi \int_0^\pi k(\theta) \, k(\arccos(\sin\theta \sin\eta \cos\phi + \cos\theta \cos\eta)) \; \mathrm{d}\phi \; \sin\eta \; \mathrm{d}\eta, \qquad 0 \le \theta \le \pi, \quad (2.3)$$

is the correlation function of the random field X. In particular, the correlation structure does not depend on the choice of the Lévy basis.

3 Hausdorff dimension

The Hausdorff dimension of a set $Z \subset \mathbb{R}^d$ is defined as follows (Hausdorff, 1919; Falconer, 1990). For $\epsilon > 0$, an ϵ-cover of Z is a finite or countable collection $\{B_i : i = 1, 2, \ldots\}$ of balls $B_i \subset \mathbb{R}^d$ of diameter $|B_i|$ less than or equal to ϵ that covers Z. With

$$H^\delta(Z) = \lim_{\epsilon \to 0} \inf \left\{ \sum |B_i|^\delta : \{B_i : i = 1, 2, \ldots\} \text{ is an } \epsilon\text{-cover of } Z \right\}$$

denoting the δ-dimensional Hausdorff measure of Z, there exists a unique nonnegative number δ_0 such that $H^\delta(Z) = \infty$ if $\delta < \delta_0$ and $H^\delta(Z) = 0$ if $\delta > \delta_0$. This number δ_0 is the Hausdorff dimension of the point set Z.

For the remainder of the section, we assume that the Lévy basis Γ is the Gaussian basis (2.1). Then X has Gaussian finite dimensional distributions and thus is a Gaussian process. While there is a wealth of results on the Hausdorff dimension of the graphs of stationary Gaussian random fields on Euclidean spaces, which is determined by the infinitesimal behaviour of the correlation function at the origin, as formalised by the fractal index (Hall and Roy, 1994; Adler, 2009), we are unaware of any extant results for the graphs of random fields on spheres, or for the surfaces of star-shaped random particles.

We now state and prove such a result. Toward this end, we say that an isotropic random field X on the sphere with correlation function $C : [0, \pi] \to \mathbb{R}$ has fractal index $\alpha > 0$ if there exists a constant $c_0 > 0$ such that

$$C(0) - C(\theta) \sim c_0 \, \theta^\alpha \quad \text{as} \quad \theta \downarrow 0. \tag{3.1}$$

The fractal index exists for essentially all correlation functions of practical interest, and it is always true that $\alpha \in (0, 2]$. The following theorem relates the Hausdorff dimension of the graph of an isotropic Gaussian random field X on the sphere $\mathbb{S}^2$ to its fractal index. The proof employs stereographic projections that allow us to draw on classical results in the Euclidean case.

Theorem 3.1. *Let X be an isotropic Gaussian random field on $\mathbb{S}^2$ with fractal index $\alpha \in (0, 2]$. Consider the random surface*

$$Z_c = \big\{ (u, X_c(u)) : u \in \mathbb{S}^2 \big\},$$

where $X_c(u) = \max(c, X(u))$ with $c > 0$. Then with probability one either of the following alternatives holds:

(a) If $\max_{u \in \mathbb{S}^2} X(u) \le c$, the realisation of Z_c is the sphere with radius c and so its Hausdorff dimension is 2.

(b) If $\max_{u \in \mathbb{S}^2} X(u) > c$, the realisation of Z_c has Hausdorff dimension $3 - \frac{\alpha}{2}$.

Proof. The claim in alternative (a) is trivial. To prove the statement in alternative (b), we assume without loss of generality that $X(u_0) > c$, where $u_0 = (0, 0, 1)$. The sample paths of X are continuous almost surely according to Gangolli (1967, Theorem 7.2). Thus, there exists an $\epsilon \in (0, \frac{1}{2})$ such that $X(u) > c$ for u in the spherical cap $\mathbb{S}^2_\epsilon = \{u \in \mathbb{S}^2 : d(u, u_0) \le \epsilon\}$ of radius ϵ centred at u_0. Let $\Pi : \mathbb{S}^2_\epsilon \to \mathbb{B}_\epsilon$ denote a stereographic projection that maps $(0, 0, 1)$ to $(0, 0)$, where $\mathbb{B}_\epsilon = \{x = (x_1, x_2) \in \mathbb{R}^2 : x_1^2 + x_2^2 \le \epsilon^2\}$. A stereographic projection is a local diffeomorphism, Π thus is differentiable and has a differentiable inverse Π^{-1}, which is locally bi-Lipschitz (do Carmo, 1976). We may therefore assume that ϵ is small enough so that for all $x, x' \in \mathbb{B}_\epsilon$ there exists a constant $A \ge 1$ with

$$\tfrac{1}{A} \|x - x'\| \le \|\Pi^{-1}(x) - \Pi^{-1}(x')\| \le A \|x - x'\|, \tag{3.2}$$

where $\|\cdot\|$ denotes the Euclidean norm on $\mathbb{R}^2$ or $\mathbb{R}^3$, respectively. Let the Gaussian random field W on $\mathbb{B}_\epsilon \subset \mathbb{R}^2$ be given by $W(x) = X(\Pi^{-1}(x))$. From Xue and

Xiao (2009, Theorem 5.1), the graph $\mathrm{Gr}\, W = \{(x, W(x)) : x \in \mathbb{B}_\epsilon\}$ has Hausdorff dimension $3 - \frac{\alpha}{2}$ almost surely if there exists a constant $M_0 > 1$ such that

$$\frac{1}{M_0} \sum_{j=1}^{2} |x_j - x_j'|^\alpha \le \mathbb{E}(W(x) - W(x'))^2 \le M_0 \sum_{j=1}^{2} |x_j - x_j'|^\alpha \tag{3.3}$$

for all $x, x' \in \mathbb{B}_\epsilon$. Letting $\vartheta(x, x') = d(\Pi^{-1}(x), \Pi^{-1}(x'))$, we have

$$\mathbb{E}(W(x) - W(x'))^2 = 2\sigma_X^2 \, [C(0) - C(\vartheta(x, x'))], \tag{3.4}$$

where $C : [0, \pi] \to \mathbb{R}$ is the correlation function of the isotropic random field X. As chord length and great circle distance are bi-Lipschitz equivalent metrics, there exists a constant $B > 1$ such that

$$\tfrac{1}{B} \, \|\Pi^{-1}(x) - \Pi^{-1}(x')\| \le \vartheta(x, x') \le B \, \|\Pi^{-1}(x) - \Pi^{-1}(x')\|. \tag{3.5}$$

As the random field X is of fractal index α, there exists a constant $M_1 > 0$ such that

$$\sum_{j=1}^{2} |x_j - x_j'|^\alpha \le 2^{1-\frac{\alpha}{2}} \|x - x'\|^\alpha \le 2^{1-\frac{\alpha}{2}} A^\alpha B^\alpha \, \vartheta(x, x')^\alpha \le M_1 \, [C(0) - C(\vartheta(x, x'))]$$

for $x, x' \in \mathbb{B}_\epsilon$ and $\epsilon > 0$ sufficiently small, where the first estimate is justified by Jensen's inequality and the second by (3.2) and (3.5). Similarly, there exists a constant $M_2 > 0$ such that

$$M_2 \, [C(0) - C(\vartheta(x, x'))] \le \sum_{j=1}^{2} |x_j - x_j'|^\alpha$$

for all $x, x' \in \mathbb{B}_\epsilon$ and $\epsilon > 0$ sufficiently small. In view of equation (3.4), this proves the existence of a constant $M_0 > 1$ such that (3.3) holds, given that $\epsilon > 0$ is sufficiently small.

Now, consider the mapping ζ from $\mathbb{B}_\epsilon \times \mathbb{R}$ to $\mathbb{S}^2_\epsilon \times \mathbb{R}$ defined by $\zeta(x, r) = (\Pi^{-1}(x), r)$, so that $\zeta(\mathrm{Gr}\, W) = \{(u, X(u)) : u \in \mathbb{S}^2_\epsilon\}$. The identity

$$\|\zeta(x, r) - \zeta(x', r')\|^2 = \|\Pi^{-1}(x) - \Pi^{-1}(x')\|^2 + |r - r'|^2.$$

along with (3.2) implies ζ to be bi-Lipschitz. Therefore by Corollary 2.4 of Falconer (1990), the partial surface $\{(u, X(u)) : u \in \mathbb{S}^2_\epsilon\}$ has Hausdorff dimension $3 - \frac{\alpha}{2}$ almost surely. Invoking the countable stability property (Falconer, 1990, p. 29), we see that the full surface $Z_c = \{(u, X_c(u)) : u \in \mathbb{S}^2_\epsilon\}$ also has Hausdorff dimension $3 - \frac{\alpha}{2}$ almost surely. □

4 Isotropic kernels

It is often important that the surface of the particle process possesses the same Hausdorff dimension as that of the real-world particles to be emulated (Mandelbrot, 1982; Orford and Whalley, 1983; Turcotte, 1987). With this in mind, we introduce and study three one-parameter families of isotropic kernels for the Lévy particle process (1.1). The families yield interesting second order structures, and we derive the asymptotic behaviour of their correlation functions at zero, which determines the Hausdorff dimension of the Gaussian particle surface.

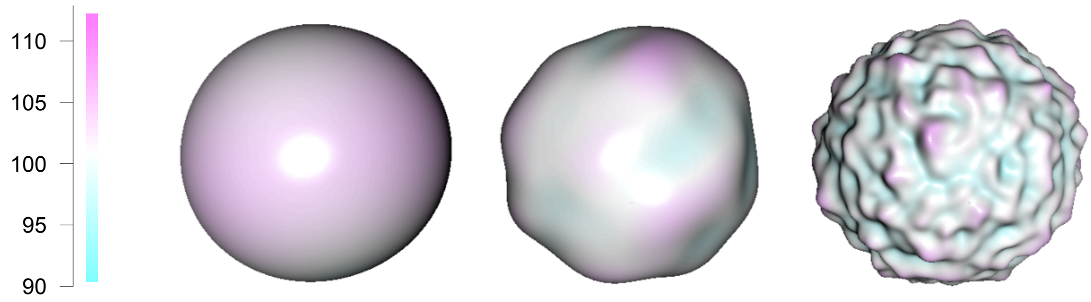

Figure 2: Lévy particles with mean $\mu_X = 100$ and variance $\sigma_X^2 = 10$, using a gamma Lévy basis and the von Mises–Fisher kernel (4.1) with $a = 3$ (left), $a = 30$ (middle) and $a = 300$ (right).

4.1 Von Mises–Fisher kernel

Here, we consider k to be the unnormalised von Mises–Fisher density,

$$k(\theta) = \mathrm{e}^{a\cos\theta}, \qquad 0 \le \theta \le \pi, \tag{4.1}$$

with parameter $a > 0$. The von Mises–Fisher density with parameter $a > 0$ is widely used in the analysis of spherical data (Fisher et al., 1987), and in this context a is called the precision.

To obtain a closed form expression for the correlation function, we consider an alternative to the representation in equation (2.3). For $\theta \in [0, \pi]$ let $u_\theta = (\sin\theta, 0, \cos\theta) \in \mathbb{S}^2$. Then

$$\begin{aligned} C(\theta) &= \frac{2}{c_2}\int_{\mathbb{S}^2} k(d(v,u_0))k(d(v,u_\theta))\,\mathrm{d}v \\ &= \frac{2}{c_2}\int_{\mathbb{S}^2} \exp\left\{a\|u_0+u_\theta\|\left(v\cdot\frac{u_0+u_\theta}{\|u_0+u_\theta\|}\right)\right\}\mathrm{d}v \\ &= \frac{4\pi}{c_2}\int_0^\pi \exp\{a\|u_0+u_\theta\|\cos\eta\}\sin\eta\,\mathrm{d}\eta \\ &= \frac{8\pi}{c_2}\,\frac{\sinh(a\|u_0+u_\theta\|)}{a\|u_0+u_\theta\|}. \end{aligned}$$

As $\|u_1+u_2\|^2 = 2\,(1+\cos d(u_1,u_2))$ for $u_1, u_2 \in \mathbb{S}^2$, we get

$$C(\theta) = \frac{2}{\sinh(2a)}\,\frac{\sinh\left(a\sqrt{2(1+\cos\theta)}\right)}{\sqrt{2(1+\cos\theta)}}, \qquad 0 \le \theta \le \pi, \tag{4.2}$$

from which it is readily seen that the fractal index is $\alpha = 2$. The surfaces of the corresponding Gaussian Lévy particles are smooth and have Hausdorff dimension 2, independently of the value of the parameter $a \in \mathbb{R}$, as illustrated in Figure 2.

4.2 Uniform kernel

We now let the kernel k be uniform, in that

$$k(\theta) = \mathbb{1}(\theta \le r), \qquad 0 \le \theta \le \pi, \tag{4.3}$$

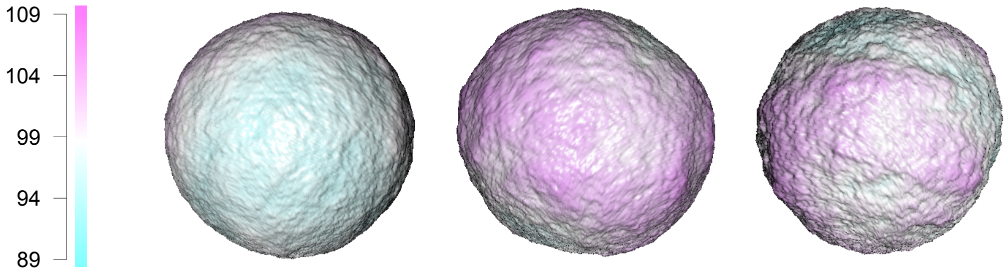

Figure 3: Lévy particles with mean $\mu_X = 100$ and variance $\sigma_X^2 = 10$, using a Gaussian Lévy basis and the uniform kernel (4.3) with $r = 1.5$ (left), $r = 1.0$ (middle) and $r = 0.5$ (right). The fractal or Hausdorff dimension of the particle surfaces equals 2.5.

with cut-off parameter $r \in (0, \frac{\pi}{2}]$. As shown in the appendix of Tovchigrechko and Vakser (2001), the associated correlation function is

$$\begin{aligned} C(\theta) = {} & \frac{1}{\pi\,(1-\cos r)} \Big(\pi - \arccos\big(\cos\theta\csc^2 r - \cot^2 r\big) \\ & - 2\cos r \arccos\left(\csc\theta\cos r\csc r - \cot\theta\cot r\right)\Big)\mathbb{1}(\theta \le 2r), \qquad 0 \le \theta \le \pi. \end{aligned} \tag{4.4}$$

In particular, if $r = \frac{\pi}{2}$ then $C(\theta) = 1 - \frac{\theta}{\pi}$ decays linearly throughout. Taylor expansions imply that the correlation function has fractal index $\alpha = 1$ for all $r \in (0, \frac{\pi}{2})$, so that the corresponding Gaussian Lévy particles have non-smooth boundaries of Hausdorff dimension $\frac{5}{2}$. Examples of Gaussian Lévy particles under this kernel are shown in Figure 3.

4.3 Power kernel

We now introduce the power kernel, which allows for Lévy particles with boundaries of any desired Hausdorff dimension. Specifically, let the isotropic kernel k be defined as

$$k(\theta) = \left(\frac{\theta}{\pi}\right)^{-q} - 1, \qquad 0 < \theta \le \pi, \tag{4.5}$$

with power parameter $q \in (0, 1)$. The associated correlation function (2.3) takes the form

$$C(\theta) = \frac{1}{c_2}\int_0^\pi \left(\pi^q\lambda^{-q} - 1\right)\sin\lambda \int_{A(\lambda)} \left(\pi^q a(\theta,\lambda,\phi)^{-q} - 1\right)\,\mathrm{d}\phi\,\mathrm{d}\lambda, \tag{4.6}$$

where

$$a(\theta,\lambda,\phi) = \arccos(\sin\theta\sin\lambda\cos\phi + \cos\theta\cos\lambda) \tag{4.7}$$

and

$$A(\lambda) = \{\phi \in [0,\pi] : 0 < a(\theta,\lambda,\phi) \le \pi\}. \tag{4.8}$$

Figures 1 and 4 show Lévy particles under the power kernel using Gaussian and gamma bases, respectively. The surface structure for the different bases resemble each other, even though the particles exhibit more pronounced spikes under the gamma basis.

Our next result will show that the correlation function (4.6) has fractal index $\alpha = 2 - 2q$, so that the corresponding Gaussian Lévy particles have surfaces with Hausdorff dimension $2 + q$, as illustrated in Figure 1.

Theorem 4.1. *If* $0 < q < 1$, *the correlation function* (4.6) *admits the expansion*

$$C(0) - C(\theta) \sim b_q \, \theta^{2-2q} \qquad \text{as} \qquad \theta \downarrow 0, \tag{4.9}$$

where

$$b_q = 2\pi^{2q} \int_0^\infty x^{1-q} \int_0^\pi \left(x^{-q} - \left(x^2 + 1 - 2x \cos \phi\right)^{-q/2} \right) \mathrm{d}\phi \, \mathrm{d}x \in (0, \infty). \tag{4.10}$$

In particular, the correlation function has fractal index $\alpha = 2 - 2q$.

Proof. We proceed in two parts, showing first that $b_q \in (0, \infty)$, and then proving the asymptotic expansion (4.9). The claim about the fractal index then is immediate from Theorem 3.1.

To show that $b_q \in (0, \infty)$ for $q \in (0, 1)$, we prove that

$$b_q = \frac{\pi^{2q+1} \Gamma(1 - \frac{1}{2}q)}{\Gamma(\frac{1}{2}q)} \int_0^\infty t^{q-1} \left(1 - \mathrm{e}^{-t} \, {}_1F_1(1 - \tfrac{1}{2}q; 1; t)\right) \mathrm{d}_* t, \tag{4.11}$$

where $d_* t = t^{-1} \, \mathrm{d}t$ and, with $(x)_0 = 1$ and $(x)_n = x(x+1) \cdots (x+n-1)$ for $n = 1, 2, \ldots$, the classical confluent hypergeometric function (Digital Library of Mathematical Functions, 2011, Chapter 13) can be written as

$${}_1F_1(a; b; t) = \sum_{k=0}^\infty \frac{(a)_k}{(b)_k} \frac{t^k}{k!}.$$

We establish the representation (4.11) as follows. With a keen eye on the inner integral in (4.10), we note that for $x > 0$ and $\phi \in (0, \pi)$,

$$x^{-q} = (x^2)^{-q/2} = \frac{1}{\Gamma(\frac{1}{2}q)} \int_0^\infty \mathrm{e}^{-tx^2} \, t^{q/2} \, \mathrm{d}_* t,$$

and

$$(1 + x^2 - 2x \cos \phi)^{-q/2} = \frac{1}{\Gamma(\frac{1}{2}q)} \int_0^\infty \mathrm{e}^{-t(1 + x^2 - 2x \cos \phi)} \, t^{q/2} \, \mathrm{d}_* t.$$

Substituting these formulas into (4.10), and interchanging the order of the integration with respect to ϕ and t, we obtain

$$b_q = \frac{2\pi^{2q}}{\Gamma(\frac{1}{2}q)} \int_0^\infty x^{1-q} \int_0^\infty t^{q/2} \mathrm{e}^{-tx^2} \int_0^\pi \left(1 - \mathrm{e}^{-t(1 - 2x \cos \phi)}\right) \mathrm{d}\phi \, \mathrm{d}_* t \, \mathrm{d}x. \tag{4.12}$$

By well-known formulas,

$$\int_0^\pi \mathrm{e}^{t \cos \phi} \, \mathrm{d}\phi = \pi \, I_0(t) = \pi \, {}_0F_1(1; \tfrac{1}{4} t^2),$$

where I_0 denotes the modified Bessel function of the first kind of order 0, and ${}_0F_1$ is a special case of the generalised hypergeometric series (Digital Library of Mathematical Functions, 2011, formulas 10.32.1 and 10.39.9). Therefore,

$$\int_0^\pi \left(1 - \mathrm{e}^{-t(1-2x\cos\phi)}\right) \mathrm{d}\phi = \pi \left(1 - \mathrm{e}^{-t}\, {}_0F_1(1; t^2x^2)\right).$$

Substituting this result into (4.12), and interchanging the order of the integration, which is justified below, we obtain

$$b_q = \frac{2\pi^{2q+1}}{\Gamma(\frac{1}{2}q)} \int_0^\infty t^{q/2} \int_0^\infty x^{1-q}\mathrm{e}^{-tx^2} \left(1 - \mathrm{e}^{-t}\, {}_0F_1(1; t^2x^2)\right) \mathrm{d}x\, \mathrm{d}_*t. \tag{4.13}$$

With the substitution $x = u^{1/2}$, we get

$$\int_0^\infty x^{1-q}\mathrm{e}^{-tx^2}\, \mathrm{d}x = \frac{1}{2}\int_0^\infty u^{-q/2}\mathrm{e}^{-tu}\, \mathrm{d}u = \tfrac{1}{2}\, t^{\frac{1}{2}q-1}\Gamma(1 - \tfrac{1}{2}q).$$

We apply next a well-known formula for the Laplace transforms of generalised hypergeometric series (Digital Library of Mathematical Functions, 2011, formula 16.5.3) to obtain, with the substitution $x = t^{-1/2}\, u^{1/2}$,

$$\begin{aligned}\int_0^\infty x^{1-q}\, \mathrm{e}^{-tx^2}\, {}_0F_1(1; t^2x^2)\, \mathrm{d}x &= \tfrac{1}{2}\, t^{\frac{1}{2}q-1} \int_0^\infty u^{-q/2}\, \mathrm{e}^{-u}\, {}_0F_1(1; tu)\, \mathrm{d}u \\ &= \tfrac{1}{2}\, t^{\frac{1}{2}q-1}\Gamma(1 - \tfrac{1}{2}q)\, {}_1F_1(1 - \tfrac{1}{2}q; 1; t).\end{aligned}$$

Consequently, by (4.13),

$$b_q = \frac{\pi^{2q+1}\Gamma(1 - \frac{1}{2}q)}{\Gamma(\frac{1}{2}q)} \int_0^\infty t^{q-1} \left(1 - \mathrm{e}^{-t}\, {}_1F_1(1 - \tfrac{1}{2}q; 1; t)\right) \mathrm{d}_*t.$$

We verify that the latter integral converges. The function $1 - \mathrm{e}^{-t}\, {}_1F_1(1 - \frac{1}{2}q; 1; t)$ has an everywhere convergent power series with constant term 0, and then it is elementary to check that

$$\int_0^u t^{q-1} \left(1 - \mathrm{e}^{-t}\, {}_1F_1(1 - \tfrac{1}{2}q; 1; t)\right) \mathrm{d}_*t$$

converges absolutely. Next,

$$\mathrm{e}^{-t}\, {}_1F_1(1 - \tfrac{1}{2}q; 1; t) \sim \frac{1}{\Gamma(1 - \frac{1}{2}q)} t^{-q/2}$$

as $t \to \infty$ (Digital Library of Mathematical Functions, 2011, formula 13.7.1); hence, for $u > 0$,

$$\int_u^\infty t^{q-1} \left(1 - \mathrm{e}^{-t}\, {}_1F_1(1 - \tfrac{1}{2}q; 1; t)\right) \mathrm{d}_*t \sim \int_u^\infty t^{q-1} \left(1 - \frac{1}{\Gamma(1 - \frac{1}{2}q)} t^{-q/2}\right) \mathrm{d}_*t < \infty.$$

This establishes the representation (4.11).

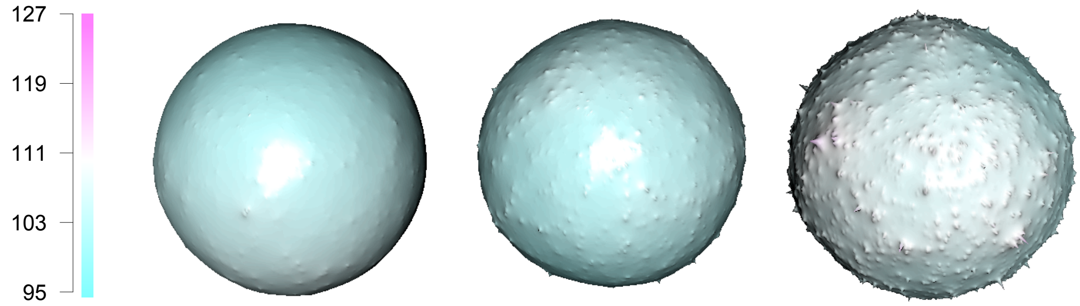

Figure 4: Lévy particles with mean $\mu_X = 100$ and variance $\sigma_X^2 = 10$, using a gamma Lévy basis and the power kernel (4.5) with $q = 0.05$ (left), $q = 0.25$ (middle) and $q = 0.5$ (right).

For $q \in (0,1)$, we have $\frac{1}{2} < 1 - \frac{1}{2}q < 1$; hence, for $k = 0, 1, 2, \ldots$,

$$0 < \frac{(1-\frac{1}{2}q)_k}{(1)_k} < 1,$$

and so we obtain

$${}_1F_1(1-\tfrac{1}{2}q; 1; t) = \sum_{k=0}^{\infty} \frac{(1-\frac{1}{2}q)_k}{(1)_k} \frac{t^k}{k!} < \sum_{k=0}^{\infty} \frac{t^k}{k!} = \mathrm{e}^t.$$

We see that $1 - \mathrm{e}^{-t}\,{}_1F_1(1-\frac{1}{2}q; 1; t) > 0$ for $t \geq 0$, and so the integrand in (4.11) is a strictly positive function. Therefore, $b_q > 0$ for $q \in (0,1)$.

Next we prove the limiting behaviour in (4.9). Let $0 \leq \theta \leq \pi$, and let the functions a and A be defined by (4.7) and (4.8), respectively. From (2.3), we get

$$\begin{aligned}
&\frac{C(0) - C(\theta)}{2} \\
&\quad = \int_0^\pi \left(\pi^q \lambda^{-q} - 1\right) \sin\lambda \left\{ \int_0^\pi \left(\pi^q \lambda^{-q} - 1\right) \mathrm{d}\phi - \int_{A(\lambda)} \left(\pi^q a(\theta,\lambda,\phi)^{-q} - 1\right) \mathrm{d}\phi \right\} \mathrm{d}\lambda.
\end{aligned}$$

Since $A(\lambda) = [0,\pi]$ for $\lambda \in (0, \pi - \theta]$ and $A(\lambda) \subset [0,\pi]$ for $\lambda \in (\pi - \theta, \pi)$, we decompose the integral on the right-hand side as $P_{1q}(\theta) + P_{2q}(\theta)$, where $P_{1q}(\theta)$ and $P_{2q}(\theta)$ correspond to the integral with respect to λ over $(0, \pi-\theta)$ and $(\pi - \theta, \pi)$, respectively.

As for the first term, substituting $\lambda = \theta x$ yields

$$\begin{aligned}
P_{1q}(\theta) &= \int_0^{\pi-\theta} \left(\pi^q \lambda^{-q} - 1\right) \sin\lambda \left\{ \int_0^\pi \left(\pi^q \lambda^{-q} - 1\right) \mathrm{d}\phi - \int_0^\pi \left(\pi^q a(\theta,\lambda,\phi)^{-q} - 1\right) \mathrm{d}\phi \right\} \mathrm{d}\lambda \\
&= \theta^{2-2q}\,\pi^{2q} \int_0^{(\pi-\theta)/\theta} \frac{\sin(\theta x)}{\theta} \left(x^{-q} - \pi^{-q}\theta^q\right) \int_0^\pi \left(x^{-q} - a(\theta, \theta x, \phi)^{-q}\theta^q\right) \mathrm{d}\phi\ \mathrm{d}x.
\end{aligned}$$

Noting that

$$\frac{\arccos(t)}{\theta} = \frac{\arccos\left(1-y^2\right)}{y} \left. \frac{y}{\theta} \right|_{y=(1-t)^{1/2}}$$

for $t \in (0,1)$, we find from (4.7) that

$$\begin{aligned}
\lim_{\theta\downarrow 0}\frac{a(\theta,\theta x,\phi)}{\theta} &= \lim_{\theta\downarrow 0}\frac{\arccos\bigl(\sin\theta\sin(\theta x)\cos\phi+\cos\theta\cos(\theta x)\bigr)}{\theta}\\
&= \frac{\mathrm{d}}{\mathrm{d}y}\arccos\left(1-y^2\right)\Big|_{y=0}\lim_{\theta\downarrow 0}\left(\frac{1-\cos\theta\cos(\theta x)}{\theta^2}-\frac{\sin\theta\sin(\theta x)}{\theta^2}\cos\phi\right)^{1/2}\\
&= \sqrt{2}\left(\frac{1+x^2}{2}-x\cos\phi\right)^{1/2}\\
&= \left(x^2+1-2x\cos\phi\right)^{1/2}.
\end{aligned}$$

An application of the Lebesgue Dominated Convergence Theorem with the dominating function

$$h(\phi,x)=\begin{cases} x^{1-q}\left(x^{-q}+1\right)\left(\left(\dfrac{x}{1-x}\right)^q+1\right), & 0<x<1,\\[2ex] x^{1-q}\left(x^{-q}+1\right)\left(\left(\dfrac{x}{x-1}\right)^q-1\right), & x>1.\end{cases}$$

shows that

$$\begin{aligned}
P_{1q}(\theta) &= \theta^{2-2q}\,\pi^{2q}\int_0^{(\pi-\theta)/\theta}\frac{\sin(\theta x)}{\theta}\left(x^{-q}-\pi^{-q}\theta^q\right)\int_0^\pi\left(x^{-q}-a(\theta,\theta x,\phi)^{-q}\theta^q\right)\mathrm{d}\phi\,\mathrm{d}x\\
&\sim \theta^{2-2q}\,\pi^{2q}\int_0^\infty x^{1-q}\int_0^\pi\left(x^{-q}-\left(x^2+1-2x\cos\phi\right)^{-q/2}\right)\mathrm{d}\phi\,\mathrm{d}x = b_q\,\theta^{2-2q}
\end{aligned}$$

as $\theta\downarrow 0$, with the strictly positive constant b_q of equation (4.10).

As regards the second term, the first mean value theorem for integration implies that there exists a $t\in(\pi-\theta,\pi)$ such that

$$\begin{aligned}
P_{2q}(\theta) &= \int_{\pi-\theta}^\pi\left(\pi^q\lambda^{-q}-1\right)\sin\lambda\left\{\int_0^\pi\left(\pi^q\lambda^{-q}-1\right)\mathrm{d}\phi-\int_{A(\lambda)}\left(\pi^q a(\theta,\lambda,\phi)^{-q}-1\right)\mathrm{d}\phi\right\}\mathrm{d}\lambda\\
&= \theta\left(\pi^q t^{-q}-1\right)\sin t\left\{\int_0^\pi\left(\pi^q t^{-q}-1\right)\mathrm{d}\phi-\int_{A(t)}\left(\pi^q a(\theta,t,\phi)^{-q}-1\right)\mathrm{d}\phi\right\}.
\end{aligned}$$

Hence, $P_{2q}(\theta)$ decays faster than $\mathcal{O}(\theta^2)$ as $\theta\downarrow 0$, which completes the proof of the asymptotic expansion (4.9). □

It is natural to look for an explicit formula for the constant b_q in equation (4.10). To that end, we apply the Kummer formula for the ${}_1F_1$ function (Digital Library of Mathematical Functions, 2011, formula 13.2.39) to show that

$$\begin{aligned}
1-\mathrm{e}^{-t}{}_1F_1(1-\tfrac{1}{2}q;1;t) &= 1-{}_1F_1(\tfrac{1}{2}q;1;-t) = -\sum_{k=1}^\infty\frac{(\frac{1}{2}q)_k}{k!}\frac{(-t)^k}{k!}\\
&= \tfrac{1}{2}qt\sum_{k=0}^\infty\frac{(\frac{1}{2}q+1)_k\,(1)_k}{(2)_k\,(2)_k}\frac{(-t)^k}{k!} = \tfrac{1}{2}qt\,{}_2F_2(\tfrac{1}{2}q+1,1;2,2;-t).
\end{aligned}$$

Thus, by the representation (4.11),

$$b_q = \frac{\pi^{2q+1} q}{2} \frac{\Gamma(1 - \frac{1}{2}q)}{\Gamma(\frac{1}{2}q)} \int_0^\infty t^q \, {}_2F_2(\tfrac{1}{2}q + 1, 1; 2, 2; -t) \, \mathrm{d}_* t,$$

and this integral is a well-known Mellin transform; see Digital Library of Mathematical Functions (2011, formula 16.5.1), where the integral is given in inverse Mellin transform format (Digital Library of Mathematical Functions, 2011, Section 1.14(iv)). We obtain

$$b_q = \frac{\pi^{2q+1}}{(1-q)^2} \frac{\Gamma(1 - \frac{1}{2}q)^2 \, \Gamma(q)}{\Gamma(\frac{1}{2}q)^2 \, \Gamma(1-q)}. \tag{4.14}$$

The power kernel (4.5) has a negative exponent and thus is unbounded. While positive exponents are feasible, they are of less interest, as the associated correlation functions have fractal index $\alpha = 2$, thereby generating smooth particles only.

5 Examples

Here, we demonstrate the flexibility of the Lévy particle framework in simulation examples. First, we introduce a simulation algorithm. Then we simulate celestial bodies whose surface properties resemble those of Earth, Moon, Mars and Venus, as reported in the planetary physics literature. Furthermore, we study and simulate the planar Lévy particles that arise from the two-dimensional version of the three-dimensional Lévy particle model (1.1).

5.1 Simulation algorithm

To sample from the Lévy particle model (1.1), we utilise the property that a Lévy basis is independently scattered. Specifically, for every sequence (A_n) of disjoint Borel subsets of $\mathbb{S}^2$, the random variables $\Gamma(A_n)$, $n = 1, 2, \ldots$ are independent and $\Gamma(\cup A_n) = \sum \Gamma(A_n)$ almost surely (Jónsdóttir et al., 2008). Let $(A_n)_{n=1}^N$ denote an equal area partition of $\mathbb{S}^2$, so that $\lambda(A_n) = 4\pi/N$ for $n = 1, \ldots, N$. The random field X in (1.1) can then be decomposed into a sum of integrals over the disjoint sets A_n, in that

$$X(u) = \sum_{n=1}^N \int_{A_n} k(v, u) \, \Gamma(\mathrm{d}v), \qquad u \in \mathbb{S}^2.$$

For $n = 1, \ldots, N$ fix any point $v_n \in A_n$. We can then approximate the random field X by setting

$$x(u) = \sum_{n=1}^N k(v_n, u) \, \Gamma(A_n), \qquad u \in \mathbb{S}^2.$$

Let us denote the common distribution of $\Gamma(A_1), \ldots, \Gamma(A_N)$, which derives either (2.1) or (2.2), depending on the choice of the Lévy basis, by F_N. To simulate a realisation y of the Lévy particle Y in (1.2), we use the following algorithm.

Algorithm 1.

1. Set $M = M_1 M_2$, where M_1 and M_2 are positive integers, and construct a grid $u_1, \ldots, u_M$ on $\mathbb{S}^2$. Using spherical coordinates, let $u_m = (\theta_m, \phi_m)$ and put $\theta_m = i\pi/M_1$ and $\phi_m = 2\pi j/M_2$, where $m = iM_2 + j$ for $i = 0, 1, \ldots, M_1 - 1$ and $j = 1, \ldots, M_2$.
2. Apply the method of Leopardi (2006) to construct an equal area partition $A_1, \ldots, A_N$ of $\mathbb{S}^2$.
3. For $n = 1, \ldots, N$, let v_n have spherical coordinates equal to the mid range of the latitudes and longitudes within A_n, respectively.
4. For $n = 1, \ldots, N$, generate independent random variables Γ_n from F_N.
5. For $m = 1, \ldots, M$, set $x(u_m) = \sum_{n=1}^{N} k(v_n, u_m)\, \Gamma_n$.
6. Set y to be the convex hull of $\{(u_m, x(u_m)) : m = 1, \ldots, M\}$.

When a Gaussian Lévy basis is used, we use the aforementioned modification, in which $x(u_m)$ is replaced by $\max(c, x(u_m))$ for some $c > 0$. This simulation procedure has been implemented in R (R Development Core Team, 2009), and code is available from the authors upon request. It can be considered an analogue of the moving average method (Oliver, 1995; Cressie and Pavlicová, 2002) for simulating Gaussian random fields on Euclidean spaces. The quality of the realisations depends on the choice of M_1, M_2 and N, and the usual trade-off applies, in that large values result in accurate simulations, at the expense of prelonged run times. For the realisations in Figures 1–4, we used $M_1 = 200$, $M_2 = 400$ and $N = 10^5$.

5.2 Celestial bodies

The geophysical literature has sought to characterise the surface roughness of the Earth and other celestial bodies in the solar system via the fractal dimension of their topography (Mandelbrot, 1982; Kucinskas et al., 1992), with Turcotte (1987) arguing that the dimension is universal and equals about 2.5. Here, we provide simulated version of the planets Earth, Venus and Mars, and of the Moon, under the Lévy particle model (1.1), with k being the power kernel (4.5). We set $q = \frac{1}{2}$, which gives the desired fractal dimension for a Gaussian particle surface, and choose the parameters $\mu_\Gamma = r_0/c_1$ and $\sigma_\Gamma^2 = (d_+ - d_-)/c_2$ of the Gaussian Lévy basis (2.1) such that they correspond to reality. For this we use the information listed in Table 2, which was obtained from Price (1988), Jones and Stofan (2008) and online sources. The values concerning Earth describe 'Dry Earth'; to simulate 'Wet Earth' we make a cut-off that corresponds to the Lévy particle Y_c with truncation parameter $c = 6371$ kilometers. In our simulation algorithm, we use $M_1 = 200$, $M_2 = 400$ and $N = 10^6$ to obtain the celestial bodies in Figure 5. The corresponding radial functions along the equator are shown in Figure 6.

5.3 Planar Lévy particles

We now reduce the dimension of the Lévy particle (1.1) and consider the planar random particle

$$Y_c = \bigcup_{u \in \mathbb{S}^1} \{o + ru : 0 \le r \le \max(X(u), c)\} \subset \mathbb{R}^2.$$

Table 2: Mean radius r_0, difference d_+ between maximal and mean radius, and difference d_- between minimal and mean radius, for Venus, Dry Earth, Moon and Mars, in kilometers.

Body	Venus	Dry Earth	Moon	Mars
r_0	6051.8	6367.2	1737.1	3389.5
d_+	11.0	8.8	5.5	21.2
d_-	-3.0	-11.0	-12.0	-8.2

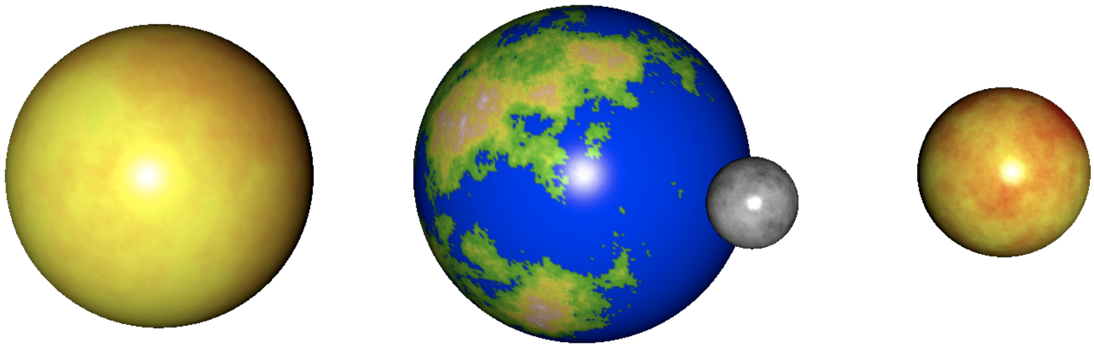

Figure 5: Simulations of Venus, Earth, Moon and Mars in true relative size.

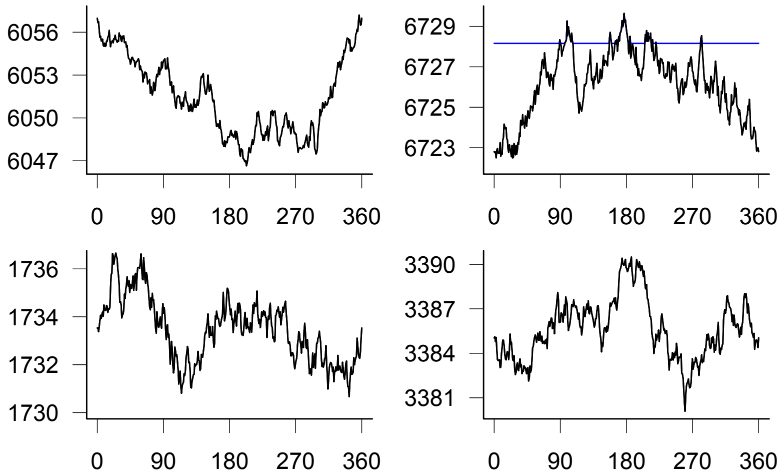

Figure 6: Radial function along the equator for the simulated bodies in Figure 5 in kilometers. Clockwise from upper left: Venus, Earth with ocean level at the blue line, Mars, and Moon.

Here $c > 0$, $o \in \mathbb{R}^2$ is an arbitrary centre, and the radial function $X(u)$ is modelled as

$$X(u) = \int_{\mathbb{S}^1} K(v,u)\, \Gamma(\,\mathrm{d}v), \qquad u \in \mathbb{S}^1,$$

with a suitable kernel function $K : \mathbb{S}^1 \times \mathbb{S}^1 \to \bar{\mathbb{R}}$ and a Lévy basis Γ on the Borel subsets of the unit sphere $\mathbb{S}^1 = \{x \in \mathbb{R}^2 : \|x\| = 1\}$. As previously, we assume that the kernel function K is isotropic, in that $K(v,u) = k(d(v,u))$ depends on the points $v, u \in \mathbb{S}^1$ through their angular or circular distance, $d(v,u) \in [0,\pi]$, only. Table 3 lists circular analogues of von Mises–Fisher, uniform and power kernels along with analytic expressions for the integrals

$$c_n = \int_{\mathbb{S}^1} k(d(v,u))^n \;\mathrm{d}v = 2 \int_0^\pi k(\eta)^n \;\mathrm{d}\eta,$$

where $n = 1, 2$, and the fractal index, α, of the associated correlation function, as defined in equation (3.1). In analogy to the respective result on $\mathbb{S}^2$, if $\max_{u \in \mathbb{S}^1} X(u) > c$, the boundary of the Gaussian Lévy particle Y_c has Hausdorff dimension $D = 2 - \frac{\alpha}{2}$ almost surely.

The general form of the associated correlation function is

$$C(\theta) = \frac{1}{c_2}\Bigg(\int_{\pi-\theta}^{\pi} k(\phi)k(2\pi - \phi - \theta)\;\mathrm{d}\phi + \int_0^{\pi-\theta} k(\phi)k(\theta+\phi)\;\mathrm{d}\phi \\ + \int_0^{\theta} k(\phi)k(\theta - \phi)\;\mathrm{d}\phi + \int_\theta^{\pi} k(\phi)k(\phi - \theta)\;\mathrm{d}\phi \Bigg), \qquad 0 \le \theta \le \pi.$$

For the von Mises–Fisher kernel with parameter $a > 0$, the correlation functions admits the closed form

$$C(\theta) = \frac{I_0\Big(a\sqrt{2(1+\cos\theta)}\Big)}{I_0(2a)}, \qquad 0 \le \theta \le \pi,$$

and for the uniform kernel with cut-off parameter $r \in (0, \frac{\pi}{2}]$, we have

$$C(\theta) = \left(1 - \frac{\theta}{2r}\right) \mathbb{1}(\theta \le 2r), \qquad 0 \le \theta \le \pi.$$

For the power kernel with parameter $q \in (0, \frac{1}{2})$, tedious but straightforward computations result in a complex closed form expression, and a Taylor expansion about the origin yields the fractal index, $\alpha = 1 - 2q$, stated in Table 3.

Thus, the von Mises–Fisher and uniform kernels result in Gaussian Lévy particles with boundaries of Hausdorff dimension 1 and $\frac{3}{2}$, respectively. Under the power kernel, the Hausdorff dimension of the Guaussian particle surface is $\frac{3}{2} + q$. Simulated planar Lévy particles using Gaussian and gamma Lévy bases with von Mises–Fisher, uniform and power kernels are shown in Figure 7, with the parameter values varying by row, as listed in Table 4. The simulation algorithm of Section 5.1 continues to apply with natural adaptions, such as defining the simulation grid $u_m = 2\pi m/M$ for $m = 1, \ldots, M$, where we use $M = 5{,}000$ and $N = 10^5$.

Table 3: Analytic form, parameter range, constants and associated fractal index for parametric familes of isotropic kernels $k : [0, 2\pi) \to \bar{\mathbb{R}}$ on the circle $\mathbb{S}^1$.

Kernel	von Mises–Fisher	Uniform	Power
Analytic Form	$k(\theta) = \mathrm{e}^{a \cos \theta}$	$k(\theta) = \mathbb{1}(\theta \leq r)$	$k(\theta) = \left(\frac{\theta}{\pi}\right)^{-q} - 1$
Parameter	$a > 0$	$r \in (0, \frac{\pi}{2}]$	$q \in (0, \frac{1}{2})$
c_1	$2\pi I_0(a)$	$2r$	$2\pi \dfrac{q}{1-q}$
c_2	$2\pi I_0(2a)$	$2r$	$4\pi \dfrac{q^2}{1 - 3q + 2q^2}$
Fractal Index	2	1	$1 - 2q$

Table 4: Values of the parameter a for the von Mises–Fisher kernel, the parameter r for the uniform kernel, and the parameter q for the power kernel used to generate the planar particles in Figure 7.

Row	a	r	q
1	3	1.5	0.05
2	30	1.0	0.25
3	300	0.5	0.45

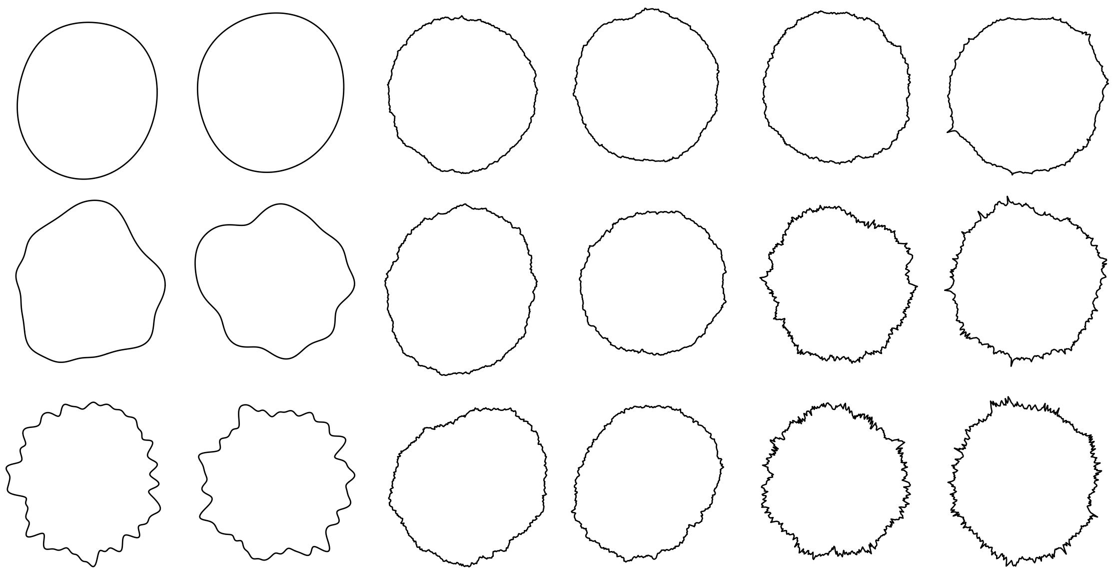

Figure 7: Planar Lévy particles with mean $\mu_X = 25$ and variance $\sigma_X^2 = 10$. Columns 1 and 2 show particles generated using a von Mises–Fisher kernel, columns 3 and 4 particles using a uniform kernel, and columns 5 and 6 particles using a power kernel, with parameters varying by row as described in Table 4. The particles in columns 1, 3, and 5 are generated under a Gaussian Lévy basis, those in columns 2, 4, and 6 under a gamma basis.

6 Discussion

We have proposed a flexible framework for modelling and simulating star-shaped random particles. The particles are represented by their radial function, which is generated by an isotropic kernel smoothing of a Lévy basis on the sphere. For Gaussian particles, the Hausdorff dimension of the particle surface depends on the behaviour of the associated isotropic correlation function at the origin, as quantified by the fractal index. Using power kernels, we obtain three-dimensional Gaussian particles with surfaces of any desired Hausdorff dimension between 2 and 3. While a non-Gaussian theory remains elusive, we believe that similar results hold for gamma particles.

We have focused on three-dimensional particles, except for an aside on planar particles in the preceding section. However, the Lévy particle approach generalises readily, to yield star-shaped random particles in $\mathbb{R}^d$ for any $d \geq 2$. The particles are represented by their radial function and associated with an isotropic random field on the sphere $\mathbb{S}^{d-1}$. In this setting, Estrade and Istas (2010) derive a recursion formula that yields closed form expressions for the isotropic correlation function on $\mathbb{S}^{d-1}$ that arises under a uniform kernel. In analogy to terminology used in the Euclidean case (Gneiting, 1999), we refer to this correlation function as the 'spherical hat' function with cut-off parameter $r \in (0, \frac{\pi}{2}]$. Any spherical hat function has a linear behaviour at the origin, and thus has fractal index $\alpha = 1$. Estrade and Istas (2010) also show that scale mixtures of the spherical hat function provide correlation functions of any desired fractal index $\alpha \in (0, 1]$, similarly to the corresponding results of Hammersley and Nelder (1955) and Gneiting (1999) in the Euclidean case.

A far-reaching, natural extension of our approach uses non-isotropic kernels to allow for multifractal Lévy particles, where the roughness properties and the Hausdorff dimension may vary locally on the particle surface. This fits the framework of Gagnon et al. (2006), who argue that the topography of Earth is multifractal, and allows for multifractal simulations of three-dimensional celestial bodies, as opposed to extant work that applies to the topography of 'Flat Earth'.

We have not dicussed parameter estimation under our modelling approach, and plan to do so in future work. In a Bayesian setting, inference could be performed similarly to the methods developed by Wolpert and Ickstadt (1998), who use a construction akin to the random field model in (1.1) to represent the intensity measure of a spatial point process, and propose a simulated inference framework, where the model parameters, the underlying random field, and the point process are updated in turn, conditional on the current state of the other variables.

Acknowledgements

The authors thank Anders Rønn-Nielsen, Eva B. Vedel Jensen, Jens Ledet Jensen, Richard Askey, and Werner Ehm for comments and discussions. Special thanks go to Donald Richards for showing us in great detail how to prove the positivity of the constant b_q in Theorem 4.1 and derive the explicit formula (4.14). This research has been supported by the Centre for Stochastic Geometry and Advanced Bioimaging at

Aarhus University which is funded by a grant from the Villum Foundation, by the Alfried Krupp von Bohlen und Halbach Foundation, and by the German Research Foundation (DFG) within the programme "Spatio-/Temporal Graphical Models and Applications in Image Analysis", grant GRK 1653.

References

Adler, R. J. (2009). *The Geometry of Random Fields* (SIAM Classics ed.). SIAM, Philadelphia.

Cressie, N. and M. Pavlicová (2002). Calibrated spatial moving average simulations. *Statistical Modelling 2*, 267–279.

Cruz-Orive, L. M. (1976). Particle size-shape distributions: The general spheroid problem. I. Mathematical model. *Journal of Microscopy 107*, 235–253.

Cruz-Orive, L. M. (1978). Particle size-shape distributions: The general spheroid problem. II. Stochastic model and particle guide. *Journal of Microscopy 112*, 153–167.

Digital Library of Mathematical Functions (2011). Release 2011-07-01, `http://dlmf.nist.gov`.

do Carmo, M. P. (1976). *Differential Geometry of Curves and Surfaces.* Prentice-Hall, Englewood Cliffs.

Estrade, A. and J. Istas (2010). Ball throwing on spheres. *Bernoulli 16*, 953–970.

Falconer, K. (1990). *Fractal Geometry.* John Wiley and Sons, Chichester.

Fisher, N. I., B. J. J. Embleton, and T. Lewis (1987). *Statistical Analysis of Spherical Data.* Cambridge University Press, Cambridge.

Gagnon, J.-S., S. L. Lovejoy, and D. Schertzer (2006). Multifractal earth topography. *Nonlinear Processes in Geophysics 13*, 541–570.

Gangolli, R. (1967). Positive definite kernels on homogeneous spaces and certain stochastic processes related to Lévy's Brownian motion of several parameters. *Annales de l'Institut Henri Poincaré section B 3*, 121–226.

Gneiting, T. (1999). Radial positive definite functions generated by Euclid's hat. *Journal of Multivariate Analysis 69*, 88–119.

Grenander, U. and M. I. Miller (1994). Representations of knowledge in complex systems. *Journal of the Royal Statistical Society Series B 56*, 549–603.

Hall, P. and R. Roy (1994). On the relationship between fractal dimension and fractal index for stationary stochastic processes. *Advances in Applied Probability 4*, 241–253.

Hammersley, J. M. and J. A. Nelder (1955). Sampling from an isotropic Gaussian process. *Proceedings of the Cambridge Philosophical Society 51*, 652–662.

Hausdorff, F. (1919). Dimension und äußeres Maß. *Mathematische Annalen 79*, 157–179.

Hellmund, G., M. Prokešová, and E. B. V. Jensen (2008). Lévy based Cox point processes. *Advances in Applied Probability 40*, 603–629.

Hobolth, A. (2003). The spherical deformation model. *Biostatistics 4*, 583–595.

Hobolth, A., J. T. Kent, and I. L. Dryden (2002). On the relation between edge and vertex modelling in shape analysis. *Scandinavian Journal of Statistics 29*, 355–374.

Hobolth, A., J. Pedersen, and E. B. V. Jensen (2003). A continuous parametric shape model. *Annals of the Institute of Statistical Mathematics 55*, 227–242.

Jones, R. H. (1963). Stochastic processes on a sphere. *Annals of Mathematical Statistics 34*, 213–218.

Jones, T. and E. Stofan (2008). *Planetology: Unlocking the Secrets of the Solar System.* National Geographic Society, Washington, D.C.

Jónsdóttir, K. Y., J. Schmiegel, and E. B. V. Jensen (2008). Lévy based growth models. *Bernoulli 14*, 62–90.

Kent, J. T., I. L. Dryden, and C. R. Anderson (2000). Using circulant symmetry to model featureless objects. *Biometrika 87*, 527–544.

Kucinskas, A. B., D. L. Turcotte, J. Huang, and P. G. Ford (1992). Fractal analysis of Venus topography in Tinatin Planitia and Ovda Regio. *Journal of Geophysical Research 97*, 13635–13641.

Leopardi, P. (2006). A partition of the unit sphere into regions of equal area and small diameter. *Electronic Transactions on Numerical Analysis 25*, 309–327.

Mandelbrot, B. B. (1982). *The Fractal Geometry of Nature.* W. H. Freeman and Company, New York.

Miller, M. I., S. Joshi, D. R. Maffitt, J. G. Mcnally, and U. Grenander (1994). Membranes, mitochondria and amoebae: Shape models. *Journal of Applied Statistics 21*, 141–163.

Muinonen, K., T. Nousiainen, P. Fast, K. Lumme, and J. I. Peltoniemi (1996). Light scattering by Gaussian random particles: Ray optics approximation. *Journal of Quantitative Spectroscopy and Radiative Transfer 55*, 577–601.

Muñoz, O., H. Volten, J. W. Hovenier, T. Nousiainen, K. Muinonen, D. Guirado, F. Moreno, and L. B. F. M. Waters (2007). Scattering matrix of large Saharan dust particles: Experiments and computations. *Journal of Geophysical Research 112*, D13215.

Oliver, D. S. (1995). Moving averages for Gaussian simulation in two and three dimensions. *Mathematical Geology 27*, 939–960.

Orford, J. D. and W. B. Whalley (1983). The use of the fractal dimension to quantify the morphology of irregular-shaped particles. *Sedimentology 30*, 655–668.

Price, F. (1988). *The Moon Observer's Handbook.* Cambridge University Press, Cambridge.

R Development Core Team (2009). *R: A Language and Environment for Statistical Computing.* Vienna, Austria: R Foundation for Statistical Computing.

Tovchigrechko, A. and I. A. Vakser (2001). How common is the funnel-like energy landscape in protein-protein interactions? *Protein Science 10*, 1572–1583.

Turcotte, D. L. (1987). A fractal interpretation of topography and geoid spectra on the Earth, Moon, Venus, and Mars. *Journal of Geophysical Research 92*, E597–E601.

Wicksell, S. D. (1925). The corpuscle problem. A mathematical study of a biometric problem. *Biometrika 17*, 84–89.

Wicksell, S. D. (1926). The corpuscle problem. Second memoir. Case of ellipsoidal corpuscles. *Biometrika 18*, 152–172.

Wolpert, R. L. and K. Ickstadt (1998). Poisson/gamma random field models for spatial statistics. *Biometrika 85*, 251–267.

Xue, Y. and Y. Xiao (2009). Fractal and smoothness properties of space-time Gaussian models. Preprint, `http://arxiv.org/abs/0912.0285`.